TECHNICAL PAPER

JOURNAL OF THE SOUTH AFRICAN INSTITUTION OF CIVIL ENGINEERING
ISSN 1021-2019 (print) | ISSN 2309-8775 (online)
Vol 67 No 3, December 2025, Pages 2–17, Paper 1758

Physical model study of novel deflector forms on uncontrolled spillways

HJ Wright, A Bosman, I Brink

Spillways are designed to control the release of excess water from a reservoir and safely convey it downstream to prevent overtopping and structural failure. The field of stepped spillways hydraulics has seen extensive research, yet several fundamental hydraulic aspects remain inadequately explored. Notably, the elusive safe unit discharge limits for these spillways remain a subject of contention within the existing literature. This paper discusses an investigation into the feasibility of novel deflector forms aimed at increasing the safe discharge capacity of uncontrolled spillways by deflecting the flow away from the spillway slope. A 1:50 scale physical model was constructed to investigate the influence of different deflector forms. The investigation spans a range of prototype unit discharges ranging from 50 $m^3/s/m$ to 200 $m^3/s/m$ and evaluates factors such as water surface profiles created by the deflector and pressure distribution on the deflector. The proposed novel deflectors developed in this study proved to be effective at various flow rates when the flow trajectory and threshold pressures were considered. These deflectors could be used for dams higher than 150 m and unit discharges between 100 $m^3/s/m$ and 200 $m^3/s/m$.

Keywords: spillways, unit discharge, physical model, pressure, deflector, jet trajectory

DR HENRY-JOHN WRIGHT is currently a Specialist Dam Engineer at ARQ. He holds a PhD and MSc in Civil Engineering, with a focus on spillway hydraulics. His 21 years of post-graduate engineering experience have focused mainly on the design of dams. His experience extends from planning through to construction implementation, where he has been extensively involved in the design and construction of large dams, spillway hydraulics, dam safety inspections and hydropower schemes. He serves presently on the Management Committee of SANCOLD and as South Africa's representative on ICOLD's Hydraulics for Dams Committee.

Contact details:
ARQ Consulting Engineers
Lynnwood Manor
Pretoria 0081
South Africa
henry-john@arq.co.za

Department of Civil Engineering
Stellenbosch University
Stellenbosch 7602
South Africa

DR ADÈLE BOSMAN (Pr Eng) is a Senior Lecturer in Hydraulics at Stellenbosch University, South Africa. She holds an MSc and PhD in Civil Engineering, specialising in hydraulics and rock mechanics. Her research focuses on scour and erosion downstream of dams and hydraulic structures, using both physical and numerical modelling. With over 16 years of experience in the water industry, she also serves as Acting Head of the University's Water Division, contributing to research leadership and academic governance.

Contact details:
Department of Civil Engineering
Stellenbosch University
Stellenbosch 7602
South Africa
abosman2@sun.ac.za

DR ISOBEL BRINK has worked in civil engineering as a general consulting engineer, lecturer and researcher in the field of water treatment, and academic copyeditor. After two years as a consulting engineer, she lectured in the field of water treatment for eight years at the University of Stellenbosch and supervised masters and doctoral students in various research areas, viz. stream pollutant modelling, point-of-use water treatment systems, pilot plants, and stormwater runoff quality. To date she has published 33 peer-reviewed journal articles as main or co-author. Her current interests lie in writing and editing where she works as a freelance copyeditor.

Contact details:
Department of Civil Engineering
Stellenbosch University
Stellenbosch 7602
South Africa
isobelbrink@outlook.com

INTRODUCTION

The hydraulics of stepped spillways are generally well understood, although numerous fundamental hydraulic aspects continue to be inadequately explored (Matos & Meireles 2014). These knowledge gaps encompass topics like the dynamics of aerated flow, hydraulics specific to embankment flows, the hydraulic behaviour of stepped spillways in the context of steep gravity dams, environmental considerations, and the complex interactions between turbulent cavity flow and skimming flows. Notably, the safe unit discharge limits for stepped spillways remain undefined, with reported values varying widely due to differences in experimental setups, aeration conditions, and step configurations (Boes & Minor 2000; Amador *et al* 2009; Boes 2012). While Boes and Minor (2000) reported a cavitation threshold at 25 $m^3/s/m$, Amador *et al* (2009) suggested lower safe limits, and Boes (2012) proposed higher values under specific aerated conditions. Rather than attempting to resolve these discrepancies, this study introduces an alternative design approach – deflectors – that may allow stepped spillways to safely accommodate unit discharges exceeding 100 $m^3/s/m$, where conventional stepped spillways may no longer be effective. This research builds upon previous findings (Guo *et al* 2003) by investigating a practical design solution for extending the operational range of stepped spillways beyond traditionally accepted thresholds.

Traditionally, stepped spillways have been designed for a maximum allowable unit discharge of 25 $m^3/s/m$ to 30 $m^3/s/m$ due to concerns about the risk of cavitation-induced damage (Minor 2000). Boes and Minor (2000) have reported that the critical velocity associated with cavitation onset on stepped spillways is approximately 20 m/s for a unit discharge of 25 $m^3/s/m$. Subsequent research revealed that a bottom aerator becomes imperative for unit discharges exceeding 30 $m^3/s/m$ (Boes 2012). Nevertheless, discrepancies persist, with other research findings suggesting lower safe unit discharge limits, ranging from 11.5 $m^3/s/m$ to 14 $m^3/s/m$ for step heights of 0.6 m to 1.2 m, respectively (Amador *et al* 2009). Consequently, the exact limits of stepped spillways remain unquantified.

In China, the flared gate pier (FGP) has been used on stepped spillways. These piers,

HJ Wright, A Bosman, I Brink. Physical model study of novel deflector forms on uncontrolled spillways.
J. S. Afr. Inst. Civ. Eng. 2025:67(3), Art. #1758, 16 pages. http://dx.doi.org/10.17159/2309-8775/2025/v67n3a1

The *Journal of the South African Institution of Civil Engineering*, which is distributed internationally, is a peer-reviewed, open-access journal licensed under a Creative Commons Attribution Licence (CC BY-NC-ND). Readers may therefore freely use and share the content as long as they credit the original creator and publisher, do not change the material in any way, and do not use it commercially. Copyright of this article remains with the authors.

initially designed to support the crest gates, have been customised to efficiently contract the flow into high-velocity jets. These piers have been used at, among others, the Dachaoshan Dam, a 111 m high roller compacted concrete (RCC) gravity dam in China (Guo 2012), with a maximum unit discharge design of 193 $m^3/s/m$. These piers redirect flow into high-velocity jets, achieving efficient energy dissipation without relying on the stepped spillway face (Koen 2017b). Although historically utilised exclusively with gated spillways, FGPs hold the potential to serve as deflector-type energy dissipators.

A variety of aerators have been fitted to augment stepped spillway performance (ICOLD 2017). Research on the use of aerators has been published by, among others, Pfister *et al* (2006b), Zamora *et al* (2008) and Willey *et al* (2010). Other aeration methods, such as using Roberts' crest splitters (Roberts 1977; Calitz & Basson 2018) and triangular protrusions (Wright 2010), have been successfully implemented. However, research has noted that these methods typically yield only marginal increases in the safe unit discharge of stepped spillways.

The main concern regarding stepped spillways revolves around the cavitation risk associated with high discharges. The critical cavitation parameter for stepped spillways is 0.5 compared to 0.2 observed for smooth chutes (Boes 2012), which subsequently limits the maximum allowable unit discharge. Although no cases of cavitation pitting have been reported on prototype spillways (Chanson 2015), the exact conditions under which cavitation may occur on stepped spillways remain uncertain (Frizell *et al* 2013). A case study of the Grand Ethiopian Renaissance Dam in Ethiopia showed that the dam experienced a flood equivalent to a unit discharge of 61 $m^3/s/m$, which resulted in only limited damage observed on some steps (Pietrangelli *et al* 2018). This suggests that stepped spillways may be capable of accommodating higher unit discharges than conventionally accepted.

This study investigates the feasibility of novel deflector forms to increase the safe discharge capacity of uncontrolled spillways. While stepped spillways effectively dissipate energy at moderate unit discharges, their performance diminishes at higher flow rates, necessitating alternative solutions. Deflectors are not intended to replace stepped spillway energy dissipation but rather to supplement it by reducing cavitation risks and guiding high-energy flows away from the spillway slope. Additionally, these deflectors can be applied to smooth chutes, gravity dams, and arch dams, where conventional spillway configurations may face similar limitations at extreme discharges.

Water is deflected away from the spillway slope with a deflector. Various deflector geometries were tested, and specific aspects were investigated, including determining a safe unit discharge for uncontrolled spillways when a particular deflector is used, energy dissipation, the water surface profile created by the deflector, and the deflector's pressures. A maximum unit discharge of up to 200 $m^3/s/m$ was investigated.

HISTORY OF STEPPED SPILLWAYS

According to Chanson (2002), the origins of stepped spillways can be traced back to around 1300 BC in Crete, Greece, while Roman aqueducts also incorporated several stepped cascades. During the first part of the 20th century, stepped spillways were used less frequently, as there was a tendency to use hydraulic jump stilling basins instead. However, since the 1970s there has been a notable resurgence of interest in stepped spillways. This renewed attention is attributed to the growing use of RCC and gabions as construction materials, both of which are particularly well-suited to the construction of stepped spillways. Furthermore, researchers have explored the application of stepped cascades, particularly for the protection of embankment dams, characterised by gentler slopes compared to gravity dams, which have been the subject of numerous studies (ICOLD 2017).

The hydraulic characteristics of stepped spillways in Southern Africa have been thoroughly documented by Geringer (1995). Geringer and Officer (1995) have provided more details on the hydraulic aspects of stepped spillways constructed in South Africa during the first half of the 20th century. The data shows that a maximum unit discharge of approximately 40 $m^3/s/m$ was successfully implemented at a relatively low dam height of around 60 m. No forced aeration was provided at any of the dams listed by Geringer and Officer (1995). Wright and Cameron-Ellis (2018) have documented dams with stepped spillways in Southern Africa in the two decades following the work completed by Geringer (1995). Compared to dams constructed up to 1995, the maximum unit discharge accepted was generally higher. De Hoop Dam was built with triangular protrusions to assist with energy dissipation of flow rates up to 40 $m^3/s/m$. The downstream ends of the piers at Metolong Dam were flared outwards to increase the aeration of the water as high up on the spillway as possible (Geringer *et al* 2012). This indicates that earlier dams with a height of less than 80 m had a maximum unit discharge of approximately 35 $m^3/s/m$, whereas the later dams with the same height had a maximum discharge of 65 $m^3/s/m$, neither utilising any artificial aeration.

CAVITATION RISK

General

Cavitation results from the formation of air bubbles or vapour cavities in the flow when it is subjected to reduced pressure. These bubbles later implode at positions of higher local pressure, potentially causing significant damage to concrete. This is due to both the high localised pressures involved and the nature of concrete itself, specifically where pressures induce tension forces in microfissures, which loosen the constituent particles of the concrete. Further ravelling, steel reinforcement vibration, and scour serve to exacerbate damage to the concrete, with the eventual cumulative damage overshadowing the extent of the initial cavitation damage (Falvey 1990).

The subject of cavitation is vast and has been documented in a number of widely-recognised textbooks. Falvey (1990) discusses concepts, damage, typical causes of cavitation, recommendations with respect to the design of spillways to limit cavitation, and practical methods to deal with the phenomenon. Falvey (1990) developed equations for the computation of the cavitation index (σ). For smooth spillways, it is commonly accepted that a threshold of $\sigma = 0.2$ indicates the need for an aerator at that specific location. Chadwick *et al* (2013) noted that cavitation will start to occur when the flow is inadequately aerated and the pressure measures equal to or less than 3 m absolute or -7 m atmospheric.

According to Falvey (1990), cavitation prevention methods include adjusting spillway geometry to limit the flow velocity, increase the flow pressure, or modify the flow boundary curvature. Additionally, using cavitation-resistant materials, while effective, can be costly for spillways. Aeration of the flow is another strategy, and maintaining surface finish and tolerance to ensure a lack of abrupt changes or undulations also contributes to cavitation prevention. Chanson (1994) has emphasised the importance of

the above-mentioned cavitation prevention measures and advised that cavitation damage might occur at a clear flow velocity ranging from 12 m/s to 15 m/s. To mitigate this risk, Chanson (1994) recommended decreasing the critical cavitation number by eliminating surface irregularities and directing cavitation bubble collapses away from solid boundaries, but aeration is typically used.

Therefore, care is required when designing spillways to ensure they remain cavitation free. Several methods are available to combat possible cavitation, of which providing a form of aeration is generally preferred.

Cavitation potential on stepped spillways

Several studies have examined the critical cavitation number for stepped chutes in comparison to smooth chutes. While there are diverging views on the maximum cavitation number, relevant studies have been reviewed and discussed in this section.

Boes (2012) discussed various aspects of the hydraulics of stepped spillways, noting that for a single step, the cavitation index (σ) is in the order of $\sigma = 1.0 \pm 0.1$. He further noted that, along the unaerated portion, a stepped chute would be more prone to cavitation compared to a smooth chute. When air is entrained, it is expected that the concrete surface is protected. Additionally, it is noted that a minimum of 1% of air in the water mixture should be sufficient to prevent or limit cavitation. Boes (2012) has noted the results of other recently completed studies related to cavitation, with σ in the order of 0.6 to 0.7 for steep slopes, and concluded that a limit of 0.5 is assumed for stepped chutes with a downstream slope of between 1V:2.9H ($\sigma = 19°$) to 1V:0.7H ($\sigma = 55°$). A limit unit discharge value of between 20 $m^3/s/m$ and 40 $m^3/s/m$ was proposed, and it was advised that an aerator or other artificial air entrainment mechanisms be provided upstream of the point of inception for larger discharges.

Lopardo (2002) has suggested that cavitation will occur where the minimum pressure (0.1% probability to occur) is recorded in macro-turbulent flow. Pressure measurements were used to determine where the minimum pressure is located for a given flow and chute geometry. USACE (1995, cited in Hager *et al* 2021) proposes a limit pressure head of -7 m to -8 m. Amador *et al* (2009) recommended limiting unit discharges based on the pressure fluctuations proposed by Lopardo (2002).

While Chanson (1989) states that a bottom air concentration of 1% to 2% is sufficient to reduce cavitation risk, Peterka (1953) states that 5% to 8% will avoid cavitation damage. The point upstream of the air inception point is therefore the most critical for cavitation inception. The equations to determine the distance from the point of inception (PI), as developed by Boes and Hager (2003), then indicate that the critical distance ($X_{i,crit}$) from the PI is determined to be nine times the flow depth at the PI. This proves that the downstream developing region, i.e. from the PI to $X_{i,crit}$, might also be prone to cavitation damage. Consequently, the areas upstream and downstream of the inception point carry the highest risk.

Hager *et al* (2021) note that the cavitation index is computed on smooth chutes based on hydrostatic pressure, but for stepped chutes, this method is not adequate as the pressure below the edge of the step is lower than the hydrostatic pressure. Also noteworthy is that RCC dams constructed in the last 20 to 30 years have not been tested by large floods to date. Hager *et al* (2021) conclude that the cavitation potential on a stepped chute should be investigated during the design process.

METHODS TO INCREASE UNIT DISCHARGE

Various methods to increase unit discharge over stepped spillways exist. Most pertinent of these are deflectors, aerators, Roberts' splitters, and trajectory buckets. These are briefly discussed below.

Deflectors

Several deflectors have been used as energy dissipation mechanisms. Ski jumps or flip buckets at the toe of smooth spillways have been used effectively for a few decades. These dissipators project flow away from the dam wall.

Roberts' splitter

In 1936, the Roberts' splitter was developed for the Loskop Dam in South Africa (Roberts 1977). The splitter works on the principle of bulking the solid stream of water that flows over the crest into different stream lanes. This is done by adding the stream breakers or splitters and a continuous step below the crest of the spillway. Energy loss is achieved when the different water streams collide with each other and when air is entrained. Owing to the energy loss, flood water reaches the apron of the dam at a lesser intensity. The Roberts' splitter has been used at more than 25 dams in South Africa as well as at dams worldwide (SANCOLD, 2016).

Mason (1983) studied and analysed the performance of several dams with Roberts' splitters and modified the original splitter design parameters to develop an optimised design. The area downstream of the dam toe is typically further protected by an impact apron to counter any residual energy in the spray. Mason (1983) has indicated that residual energy of as much as 30% of the height of the dam can remain in the disseminated jet in the form of dynamic pressures on the apron slab.

Calitz and Basson (2018) studied the artificial aeration of flow by adding air vents positioned on the Roberts' splitters. A 1:20 scale hydraulic model was tested with two different vent sizes and compared to an unaerated base model. The study concluded that using an internal aeration gallery can increase the unit discharge of Roberts' splitters to at least 50 $m^3/s/m$ at a head of 7.6 m, compared to the unaerated limit of 35 $m^3/s/m$. The original limits by Roberts (1977) were substantially lower, with a maximum discharge of 12 $m^3/s/m$ at a head of 3 m for an unaerated splitter. It must be noted that the Victoria and Wadi Dayqah Dams, located in Sri Lanka and Oman, respectively, have been designed with Roberts' splitters for larger unit discharges (72 $m^3/s/m$ and 84 $m^3/s/m$, respectively) than the limit proposed by Calitz and Basson (2018). Parameters of dams with unit discharges above 50 $m^3/s/m$ fitted with Roberts' splitters are listed in Table 1. Aeration facilities were provided for all these dams.

Trajectory bucket

Khatsuria (2005) noted that different names are used globally to describe structures that employ the action of jet trajectory to

Table 1 Details of dams provided with Roberts' splitters

Dam	Date	Country	Height (m)	Unit flow ($m^3/s/m$)
Gariep	1971	South Africa	75	76.0
Van der Kloof	1977	South Africa	98	57.0
Victoria	1978	Sri Lanka	101	72.3
Wadi Dayqah	2009	Oman	75	84.2

Table 2 Characteristics of various prototype flip buckets (adapted from Mason 1993)

Dam	Country	Unit flow ($m^3/s/m$)	Height from reservoir to bucket invert (m)
Brazeau	Canada	75.5	53.0
Donkarayi	India	77.3	62.5
Jaguara	Brazil	166.0	31.5
Picote	Portugal	173.0	56.0
Pine Flat	USA	125.0	113.4
Van der Kloof	South Africa	144.0	59.5

* Obtained from Back *et al* (1973)

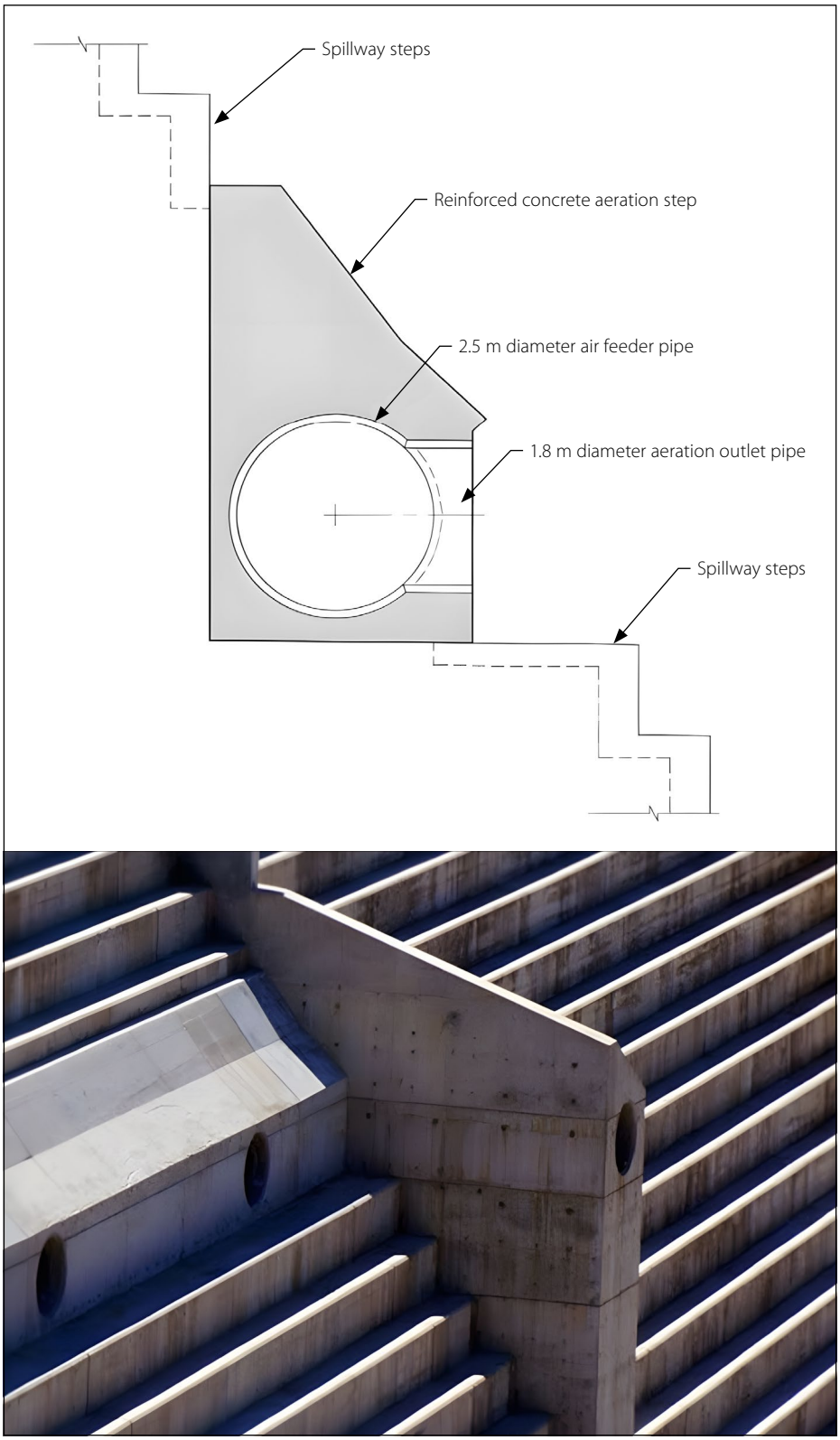

Figure 1 Aerator at enlarged Cotter Dam (Willey *et al* 2010)

accomplish energy dissipation, with the most common terminology being ski jump, flip bucket, or trajectory bucket. Heller *et al* (2005) highlighted that these structures are primarily used at the foot of a dam where the velocity exceeds 20 m/s. This guideline arises from concerns related to cavitation, abrasion, and uplift at the same velocity within stilling basins, as documented by Vischer and Hager (1995). Trajectory buckets as a type of energy dissipator were first introduced in France in the 1930s.

Schleiss (2002) noted that gated chute ski jumps nowadays are designed for unit discharges ranging from 200 $m^3/s/m$ to 300 $m^3/s/m$ because the cavitation risk of chutes is mitigated by the installation of bottom aerators. Hager *et al* (2021) cited works by Mason (1993), where it is noted that a trajectory basin or ski jump requires the following to be effective: a minimum head of 30 m and total discharge in m^3/s to be smaller than 200 $(H - H_i)$, where H is the dam height and H_i = 8 m. A unit discharge limit is not provided.

Ski jumps typically consist of an approach chute with a deflector at its end, deflecting the discharge into the air. Air is entrained into the jet during deflection, reducing its scour potential during impact downstream, typically in a plunge pool. Parameters of dams with unit discharge above 50 $m^3/s/m$ with flip buckets are listed in Table 2. The trajectory bucket can accommodate large unit discharges (above 100 $m^3/s/m$), as noted by Mason (1993). These structures have performed well on various prototypes.

Aerators

Falvey (1990), ICOLD (1992) and Khatsuria (2005) have detailed research on forced aeration on mainly smooth chutes. It has been widely accepted that the mixture of air and water absorbs cavitation impacts. Boes (2012) has also noted that for discharges of more than 30 $m^3/s/m$, a bottom aerator is required for stepped chutes.

Deflector aerator

Pfister *et al* (2006a) have studied the impact of two aerators located close to the first vertical step in order to entrain air. The first aerator was placed upstream of the first step, whereas the second aerator was placed inside the first step. The area immediately downstream of the aerator shows significant differences when compared to a standard stepped spillway.

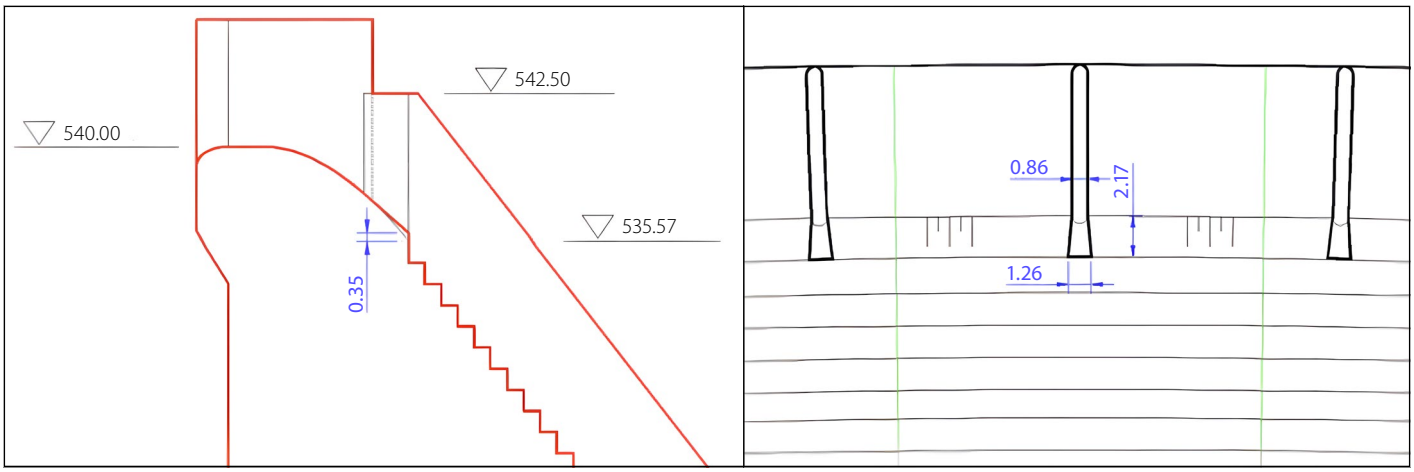

Figure 2 Aerator at Murum Dam (Ji *et al* 2014)

Step aerator

Pfister *et al* (2006b) and Zamora *et al* (2008) provided the step aerator at the first vertical face. The studies have shown that the aerator adds a small amount of air downstream of the aerator, but also that the air is quickly detrained further downstream. This increases the unit discharges considered to be safe up to 40 m^3/s/m. Larger unit discharges require the introduction of a second aerator. The aerator on a stepped chute, based on the work by Terrier (2016), is effective for flows up to 60 m^3/s/m. It is unclear how such a deflector performs at higher flows.

Examples of prototype spillways

Enlarged Cotter Dam

An aerator was developed for the Enlarged Cotter Dam in Australia as the unit discharge approached 48 m^3/s/m. A reinforced concrete aeration step with air feeder pipe and aeration outlets was incorporated. Both numerical and physical model studies were used and complemented each other to develop the complex spillway arrangement (Willey *et al* 2010). Figure 1 shows the details of the aerator.

Murum hydropower project

A 146 m high RCC gravity dam forms part of the Murum hydropower project in Malaysia. A model study at a scale of 1:40 was constructed to evaluate the behaviour of the stepped spillway, with a maximum discharge of 39.21 m^3/s/m (Wang *et al* 2012). The spillway is split into four bays, each approximately 13 m wide, with the piers used to support a bridge. A ramp at the first step 0.35 m high, as well as vertical wedges at the downstream edge on each side of the bridge piers, were also tested to address concerns regarding possible cavitation damage on the steps. Wang *et al* (2012) concluded that these additions improved the overall hydraulic behaviour of the spillway. This aerator layout is shown in Figure 2.

Boguchany Dam

Toloshinov *et al* (2009) have discussed the design of the spillway of the 79 m high Boguchany Dam in Russia, a rockfill embankment with a gravity spillway section. The maximum unit discharge applicable is 45 m^3/s/m, and there are five vertical gates for the 10 m wide openings. There are also two aerators. The first aerator is located where the smooth ogee transitions into a stepped spillway. This aerator is 1 m high and is followed by seven steps, each 0.5 m high. Thereafter, 1.5 m high steps are provided until the downstream end of the gate piers is reached. A second aerator, comprising a 3.6 m high step, is located thereafter. Sudol'skii and Volynchikov (2017) described the prototype testing of the spillway in 2015, where a maximum discharge of 17 m^3/s/m was released, indicating satisfactory hydraulic performance and no damage to the concrete steps at that flow.

De Hoop Dam

Wright (2006 and 2010) studied the installation of triangular protrusions on stepped spillways. These protrusions were constructed at the De Hoop Dam in South Africa. Hydraulic model tests indicated that they are an effective measure to increase the friction factor (slope roughness) and improve both aeration and energy dissipation. It has further been shown that triangular protrusions located on the upper part of the spillway help to shorten the length of inception (higher location of the PI) and entrain air earlier. Consequently, a spillway fitted with triangular protrusions will be effective up to 40 m^3/s/m.

Flared gate pier

The FGP was developed in China during the 1970s. It FGP is a reversal of the traditional gate pier, where the end is flared rather than having tapered tails or square ends (Lin *et al* 1987). Lin *et al* (1987) further reported that model tests have indicated less scour downstream of a stilling basin than with a traditional pier. The pier's primary function is to structurally support the crest gates, with a secondary function to contract the flow into a high-velocity jet. Figure 3 shows the typical layout of the FGP at Dachaoshan Dam. These piers have been used at, among others, the Ankang, Dachaoshan, Dichasia, Shuidong, and Suofengying Dams, all in China. In these cases, the design flood unit discharge is more than 100 m^3/s/m (Koen 2017a). Several FGPs also use slit-type flip buckets to further assist with jetting the flow away from the downstream face of the dams.

The unit discharge associated with the Dachaoshan Dam is 165 m^3/s/m for the design flood and 250 m^3/s/m for the check flood, respectively (Guo *et al* 2003). Pressure, velocity, and aeration measurements were undertaken in 2002, and revealed that the flip bucket at the end of the flaring pier gate was effective in that it allowed the main jet to flow away from the steps and, crucially, helped provide air cavities along the steps which mitigated cavitation damage. It was concluded that the air concentration was at least 30% and, therefore, the risk of cavitation damage is reduced.

EXPERIMENTAL WORK

Model scale

A physical hydraulic model is a scaled representation of a hydraulic system. A

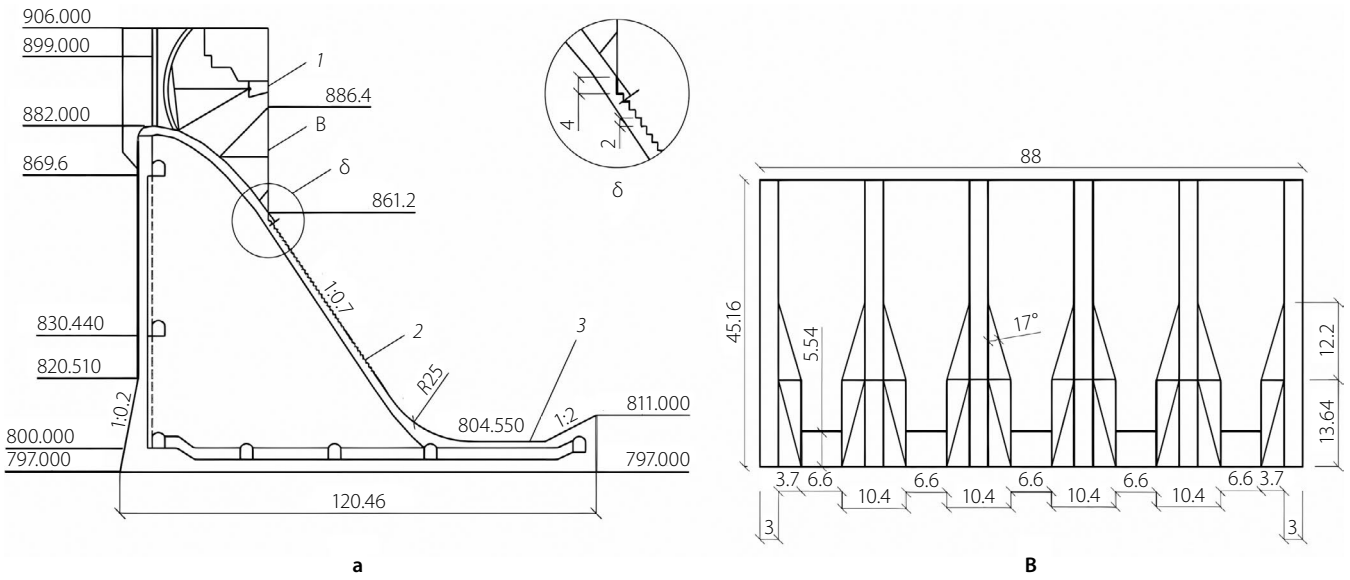

Figure 3 Schematic layout of FGP at Dachaoshan Dam: (a) dam cross-section, (b) elevation seen from the downstream side (Nan & Rumayanysev 2014)

representative scale is used, and such models are typically used during the design phases of a project to optimise and investigate critical aspects that could influence the structure. Although a powerful tool, physical models have limitations, specifically termed the effect of scale.

Boes (2000) has referred to various model studies and provided information on the scale and items tested. Not all of these model studies provided the necessary limiting Reynolds and Weber numbers. Consequently, model studies were systematically conducted at the Swiss Federal Institute of Technology, Zurich, to investigate the effect of scale. Boes (2000) concluded that to scale prototype dimensions using the Froude similarity law with negligible scale effects, the Reynolds number must be higher than 1×10^5, and the Weber number must be more than 100. When testing unit discharges of up to 20 $m^3/s/m$, a minimum scale of 1:20 to 1:15 is implied for steps 0.6 m high (Boes 2000).

Terrier (2016) has studied air-water flow on chute spillways, specifically aerators for stepped spillways. Reference is made to the Morton number, which links the Reynolds, Weber and Froude numbers. Terrier (2016) noted that scale effects will be minimised if the Reynolds number is $\geq 2 \times 10^5$ to 3×10^5 for cases where the Froude number is equal to or greater than 5.

It must be noted that available literature is generally limited to a unit discharge of about 25 $m^3/s/m$. The aim of this study was to test flows up to 200 $m^3/s/m$, which is nearly 10 times higher. This requires large laboratory pumping capacities, which is not possible in most research and commercial laboratories. Calculations were therefore performed to determine the Froude, Weber and Reynolds numbers for these larger flows. These calculations were conducted at two key locations: upstream of the uncontrolled ogee approach and at the deflector. The analysis was carried out across a range of prototype unit discharges of 50 $m^3/s/m$, 100 $m^3/s/m$, 150 $m^3/s/m$ and 200 $m^3/s/m$. Notably, the low flow rate ($q = 50\ m^3/s/m$) could potentially be influenced by scale-related effects if the work of Terrier (2016), based on research by Pfister and Chanson (2014), was considered.

The flow at the deflector location downstream of the ogee crest is however not yet aerated and consequently cannot be directly compared to the work of Terrier (2016). For this study, the Reynolds criteria ($> 2 \times 10^5$ to 3×10^5) was met, but the additional Weber number criteria (> 100) is considered to be too conservative. If both the Reynolds and Weber criteria are met, a minimum flow of 80 $m^3/s/m$ was required to limit scale effects.

The Stellenbosch University Hydraulic Laboratory has a maximum flow capacity of 600 ℓ/s. A model scale of 50 could be accommodated to test a unit discharge of 200 $m^3/s/m$. The selected scale limited the influence of surface tension to minimise any inordinately large-scale effects it might have on the air-water interface of the overflow nappe and air entrainment in the water body downstream of the deflectors. This aligns with the guidelines proposed by Boes (2000), Chanson (2009), and Hager and Boes (2014).

Model layout

The physical model of a stepped spillway capable of studying various deflectors was constructed in the Hydraulics Laboratory of the Civil Engineering Department of Stellenbosch University, illustrated in Figure 4. The model was 4 m above the laboratory floor and carried a maximum flow rate of nearly 600 ℓ/s. The construction of the 1:50 scaled model consisted of:

- An elevated rectangular horizontal approach canal, 1 m wide × 2.5 m deep × 7 m long. The canal was supported by brickwork and a steel frame.
- The approach canal was equipped with an in-flow energy absorber L-plate and flow suppressors on its upstream side. These flow suppressors reduced the turbulence caused by the large flow, upstream 90° pipe bend, and pump fluctuations.
- A steel ogee section used the USACE ogee profile.
- Wood steps, each 24 mm high and 19.2 mm horizontal (slope of 0.8 H: 1.0 V), were used on the spillway.
- One wall was made from clear Perspex to observe the flow profile, and the other from steel.
- An outflow channel from the brickwork was connected to the laboratory canal ring structure.

The deflector geometries were made from plastic and using a Creality CR 10 MAX printer. The geometric design was created in AutoCAD, and the file was exported into a format compatible with the UltiMaker Cura software. The 3D printer utilised 1.75 mm polylactic acid filament. The

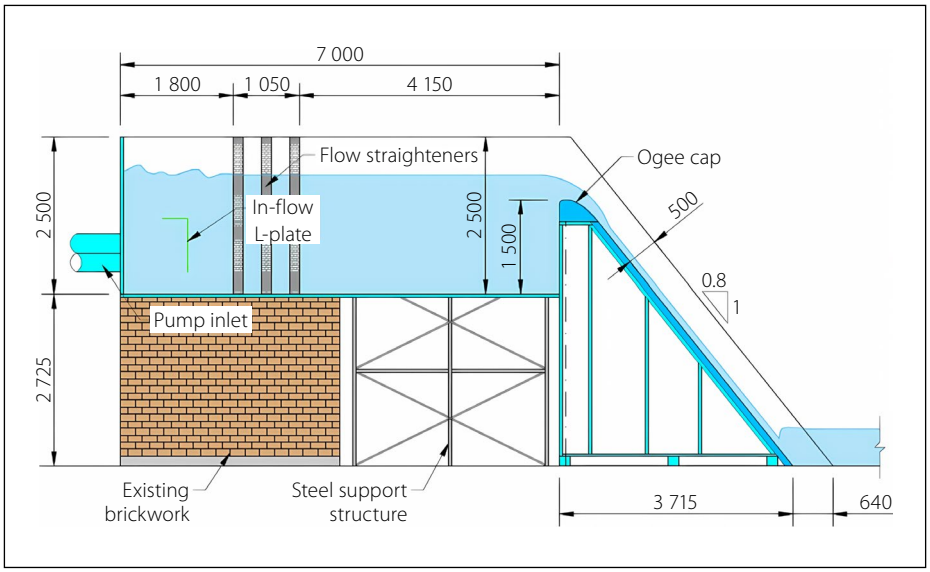

Figure 4 Schematic layout of physical model set-up

sections were modular to ensure quick fixing and removal to the main model body. A photograph of some of the units are shown in Figure 5.

Deflector geometries

The following four deflector geometries were tested, as shown in Figure 6:

- **Top row flare (Configuration 1):** The Y-shape FGP was implemented on the Dachaoshan Dam in China. No design guidelines have been disclosed, but the dimensions were obtained from Nan and Rumayanysev (2014). The total height of the flare is 25.8 m and the width is 3.7 m. These dimensions were used in the tests conducted by Koen (2017a) and Saayman (2020).
- **Flare with ski jump (Configuration 2):** The same flare with a small radius ski jump was placed between the flares. The addition of the ski jump was intended to enhance deflection, capitalising on the effects of the flares, which not only contracted the flows but also introduced aeration. This configuration yielded a more pronounced jet trajectory.
- **Triangle (Configuration 3):** A triangular deflector was designed, featuring a height equivalent to 10 steps and four complete units distributed across the modelled width. The geometry was chosen due to its ease of construction and its multifaceted impact on the flow, as it both contracts and aerates the flow while deflecting it. The results were promising, particularly in terms of enhancing aeration observed at lower flow rates. However, at higher flow rates, issues with partial submergence occurred.
- **Triangle with flare (Configuration 4):** The triangular deflector (Configuration 3) was combined with the top row flares

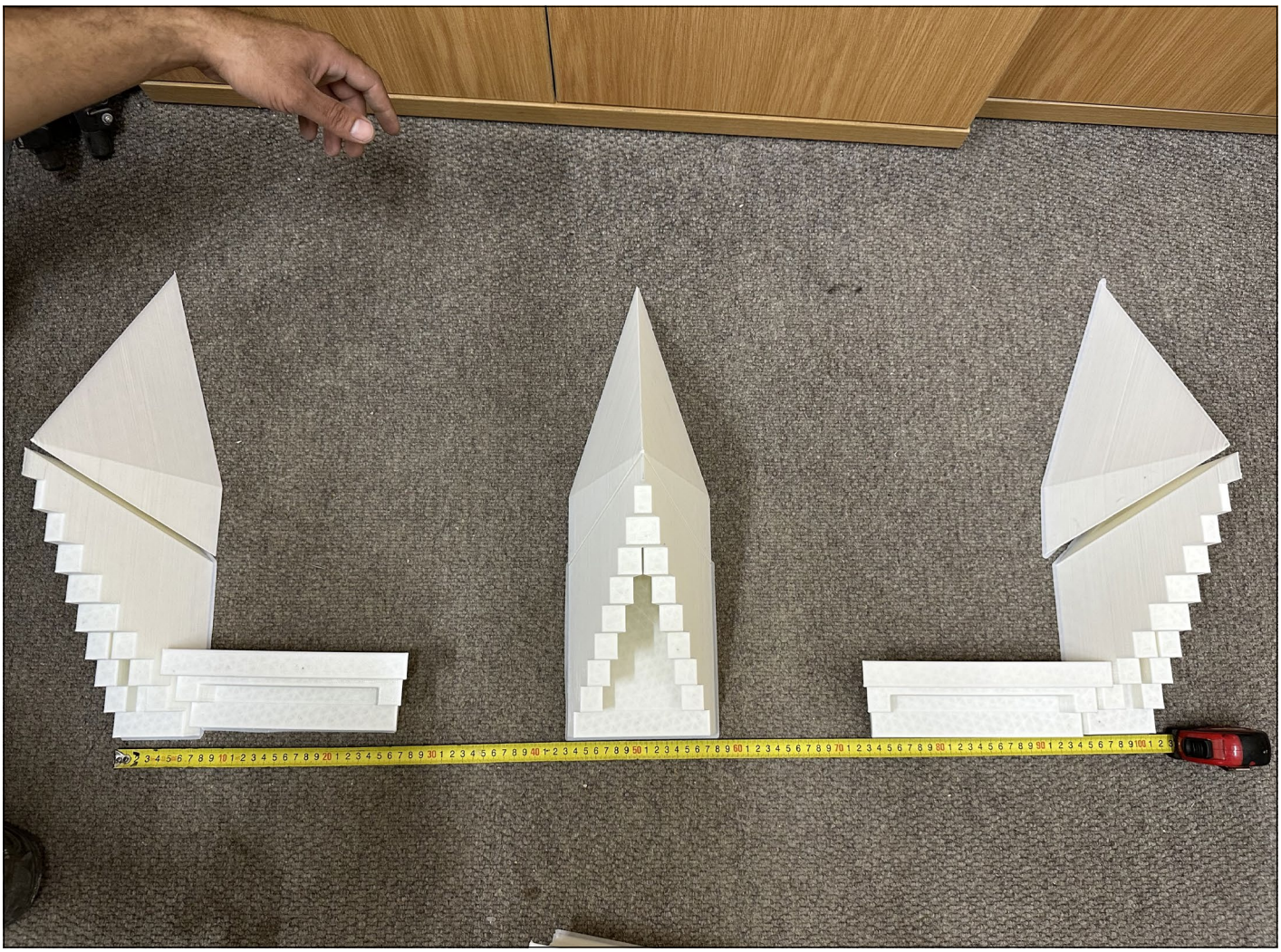

Figure 5 3D printed deflectors

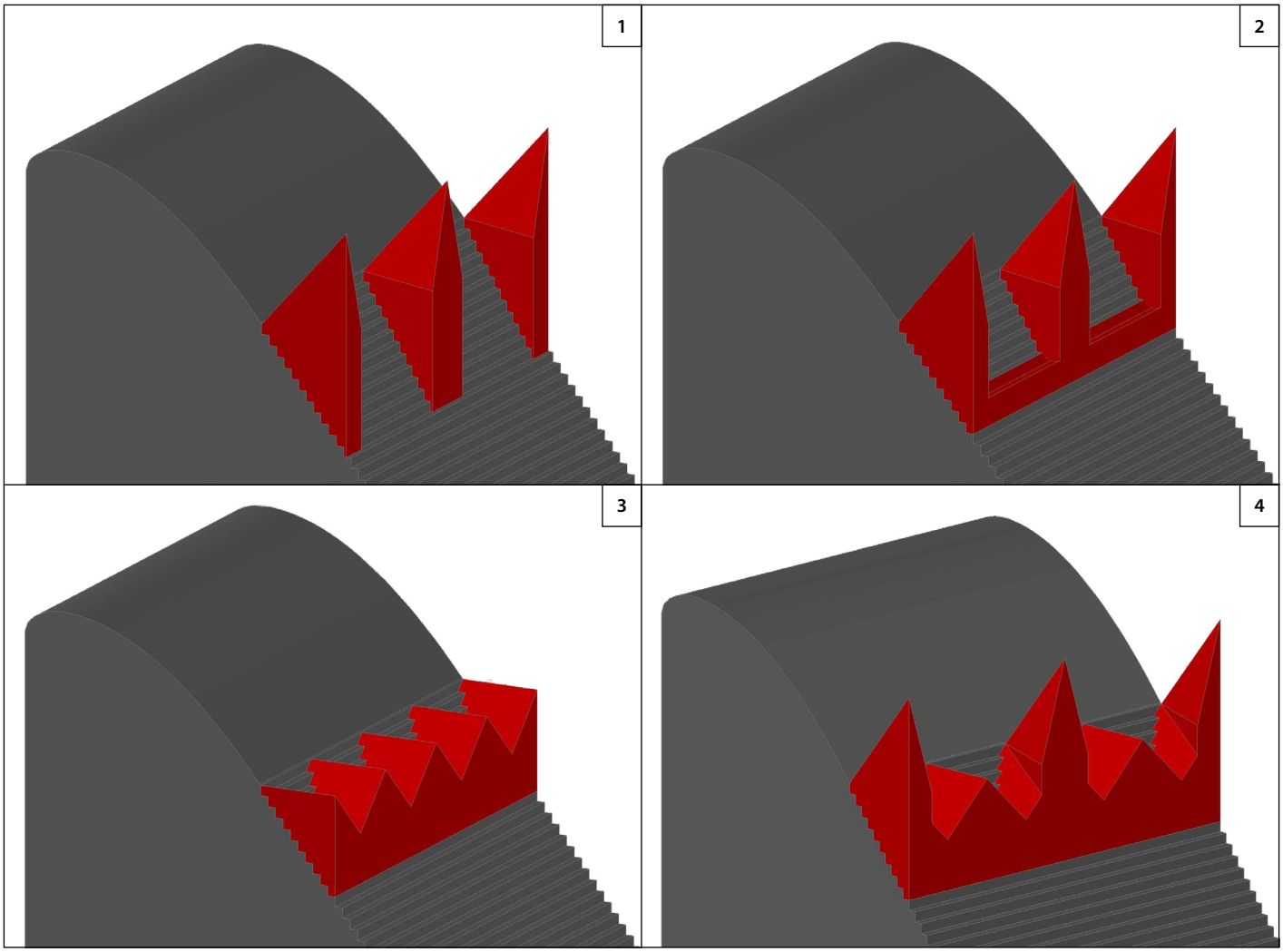

Figure 6 Deflector geometries tested

(Configuration 1). This option resulted in the further deflection of the jet compared to the other four configurations.

Results from experimental work

Sixteen complete tests were conducted on the four flares and four deflector geometries. Results of selected tests are presented in this paper since all the tests followed similar trends.

Pressure results

The pressure results for each deflector configuration are summarised in Table 3 to Table 6, and presented as prototype values in metres. The pressure profile along the deflectors was determined by measuring the dynamic flow pressures at certain strategic points. The pressure transmitters were connected to pressure taps by means of 6 mm diameter tubes of approximately 100 mm length. These taps were installed to be flush with the deflector. Pressure measurements were recorded at 100 Hz using a 16-channel analogue-to-digital data logger, ensuring a high-resolution dataset for analysis. The results, summarised in Tables 3 to 6, provide a comprehensive quantification of pressure distribution along the deflectors under varying unit discharges. This approach ensures that findings are based on detailed experimental data.

The recorded pressures indicate that most deflector configurations maintain positive pressures at critical locations, minimising cavitation risk. The only exception is Configuration 1 (top row flare) at 200 $m^3/s/m$, where localised pressures drop below -7 m. However, aeration effects and structural modifications (such as stainless steel caps) would help mitigate cavitation concerns in practice. Additionally, deflector placement ensures that they operate before cavitation inception becomes a significant risk.

These measurements represent dynamic pressures rather than purely hydrostatic values, capturing localised variations caused by high unit discharge and flow redirection. The jet trajectory results (Table 7, Figure 7) further demonstrate that deflector-induced aeration enhances air entrainment, reducing the likelihood of cavitation damage. The flow separation at the deflector edges promotes air mixing into the water jet, similar to aeration effects observed in ski jump spillways and Roberts' splitters (Boes & Hager 2003). Given these observed aeration benefits, additional aeration devices were not deemed necessary in this study. However, future research should evaluate aeration efficiency under full-scale conditions and complement these findings with numerical simulations to assess pressure distributions and potential cavitation zones under varying flow conditions.

While lower unit discharges (<50 $m^3/s/m$) were not the primary focus of this study, the observed lower pressures at reduced flows are expected due to the naturally lower kinetic energy and enhanced aeration in these conditions. At lower discharges, flow remains closer to the spillway slope, where standard stepped spillway dissipation mechanisms remain effective. Future research could explore the full performance spectrum of deflectors across a broader range of flows.

Values exceeding a negative pressure of –7 m (indicating an onset of cavitation) are noted in red, while other negative values are shaded in blue. Several observations are apparent from the pressure result analysis:

Table 3 Pressure results for top row flare (Configuration 1)

Flow ($m^3/s/m$)	Position											
	P1	P2	P3	P4	P5	P6	P7	P8	P9	P10	P11	P12
50	8.80	–2.90	3.84	3.49	–5.61	–3.42	3.45	7.43	–0.23	4.06	0.76	4.43
100	12.86	7.91	8.73	5.69	–5.85	–2.67	7.78	11.93	–3.63	6.75	0.89	5.54
150	16.86	11.58	10.59	8.47	–6.08	–1.88	11.01	12.14	–1.22	8.42	12.07	6.15
200	20.07	14.69	12.64	10.99	–5.36	–1.37	13.39	12.92	–7.55	10.75	18.16	7.62

Table 4 Pressure results for flare with ski jump (Configuration 2)

Flow ($m^3/s/m$)	Position													
	P1	P2	P3	P4	P5	P6	P7	P8	P9	P10	P11	P12	P13	P14
50	14.08	–4.06	–1.11	3.66	–3.42	19.44	3.84	7.27	17.74	6.84	17.55	20.26	14.08	17.55
100	19.13	–1.93	–6.55	10.33	4.06	24.40	9.72	13.35	14.86	13.44	21.98	24.81	19.13	21.98
150	24.70	10.73	–4.24	15.78	6.98	27.55	14.32	16.01	18.18	16.91	24.36	27.41	24.70	24.36
200	28.49	19.36	–1.15	19.36	9.39	29.98	18.06	19.29	20.28	21.15	26.27	30.61	28.49	26.27

- The top row flare option (Configuration 1) consistently exhibited the most negative pressures across the range of flow ranges tested, but only the unit discharge of 200 $m^3/s/m$ falls outside the -7 m limit.
- When comparing the top row flare (Configuration 1) with the flare ski jump (Configuration 2), it was clear that when the ski jump is added, it alters the pressures on the flare itself.
- The triangle with flare (Configuration 4) displayed low pressures, raising concerns about potential cavitation issues at the unit discharge of 50 $m^3/s/m$. This was due to possible scale effects.
- The triangle (Configuration 3) had the least negative pressures over the full spectrum, followed by the triangle with flare (Configuration 4).
- For the top row flare (Configuration 1), the most negative pressures occurred at the lower parts of the flare itself, as well as at the most downstream part for the full flare.
- At the flare with ski jump (Configuration 2), the upper part of the flare showed the most negative pressures. The ski jump has large positive pressures.
- The tip of the central triangle in Configuration 3 indicated a minor negative pressure with little risk for cavitation damage.
- At the triangle with flare (Configuration 4), the upper part of the flare was most prone to negative pressures, specifically at lower discharges.
- Contrary to expectations, there was no evident trend of increasing negative pressures with increasing flow.
- The flow is not entirely symmetrical, i.e. pressures on the left and right flare are unequal. Contraction effects are considered to contribute to this discrepancy, as well as minor construction inaccuracies.

Table 5 Pressure results for triangle (Configuration 3)

Flow ($m^3/s/m$	Position							
	P1	P2	P3	P4	P5	P6	P7	P8
50	11.48	10.47	3.72	13.32	13.28	–1.13	6.72	25.02
100	14.39	13.39	8.68	21.02	22.90	1.89	16.53	29.37
150	17.48	17.03	14.03	25.63	28.65	5.97	19.77	31.65
200	20.16	19.76	17.27	29.01	33.32	9.74	21.51	36.35

The location of the pressure measurements is included in Annexure A.

Jet trajectory

The objective was to measure the jet trajectory from the deflector end to the

Table 6 Pressure results for triangle with flare (Configuration 4)

Flow ($m^3/s/m$)	Position													
	P1	P2	P3	P4	P5	P6	P7	P8	A	B	C	D	E	F
50	19.774	16.771	1.111	13.006	9.792	–0.920	8.976	25.781	10.174	–3.385	–11.528	4.167	1.493	–7.465
100	23.193	21.788	7.066	20.990	20.191	2.760	15.208	29.740	18.785	6.962	2.153	14.427	11.510	–0.243
150	24.340	25.590	11.493	25.625	28.993	8.212	18.073	32.465	23.464	14.193	10.938	19.453	16.589	5.521
200	25.868	28.218	14.462	28.097	30.000	11.493	19.826	34.149	25.521	19.531	14.427	22.917	19.583	7.604

Table 7 Jet trajectory results

Deflector	Trajectory (m)			
	q = 50 $m^3/s/m$	q = 100 $m^3/s/m$	q = 150 $m^3/s/m$	q = 200 $m^3/s/m$
Top row flare (Configuration 1)	56.55 (1.131)	72.20 (1.444)	79.65 (1.593)	95.65 (1.913)
Flare with ski jump (Configuration 2)	119.05 (2.381)	126.90 (2.538)	126.90 (2.538)	134.70 (2.694)
Triangle (Configuration 3)	111.25 (2.225)	126.90 (2.538)	126.50 (2.530)	126.90 (2.538)
Triangle with flare (Configuration 4)	126.50 (2.530)	150.00 (3.000)	154.10 (3.082)	158.15 (3.163)

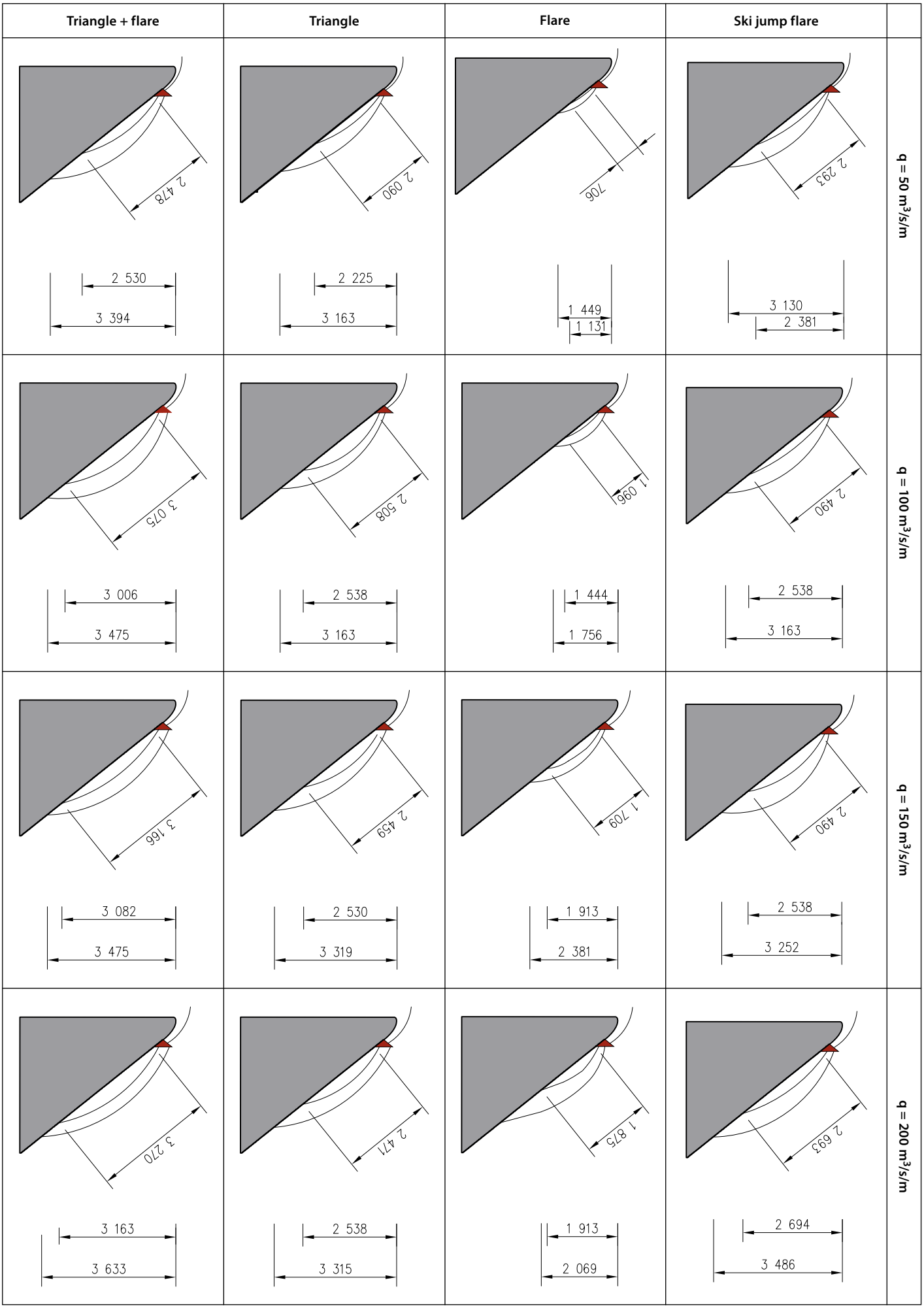

Figure 7 Jet trajectory results for model in graphical format

Table 8 Pressure criteria summary

Deflector	q = 50 m³/s/m	q = 100 m³/s/m	q = 150 m³/s/m	q = 200 m³/s/m
Top row flare (Configuration 1)	Yes	Yes	Yes	No
Flare ski jump (Configuration 2)	Yes	Yes	Yes	Yes
Triangle (Configuration 3)	Yes	Yes	Yes	Yes
Triangle with flare (Configuration 4)	No*	Yes	Yes	Yes
* Due to scale effects				

Table 9 Jet trajectory comparison to jet observed from top row flare (Configuration 1)

Deflector	Trajectory (m)			
	q = 50 m³/s/m	q = 100 m³/s/m	q = 150 m³/s/m	q = 200 m³/s/m
Flare with ski jump (Configuration 2)	211%	176%	159%	141%
Triangle (Configuration 3)	197%	176%	159%	133%
Triangle with flare (Configuration 4)	224%	208%	193%	165%

downstream slope of the spillway in order to determine an impact zone. The prototype jet trajectory for the various deflectors and flows are summarised in Table 7, with model values provided in brackets, and Figure 7. The trajectories generally increase with increasing flow rates. However, for the triangle deflector (Configuration 3), partial submergence at higher discharges resulted in reduced jet trajectory due to submergence.

The jet trajectories in graphical form as model values are shown in Figure 7.

Conclusions from results

Owing to the unique geometry of each deflector, conducting a direct one-on-one comparison among all deflectors was not feasible. To provide some common ground, the flares shared 12 measuring points across the top row flare, flare with ski jump, and triangle with flare configurations. However, in the case of the triangle with flare configuration, only six of the 12 measuring points overlapped, as the triangle portion closed off the bottom three points. The triangle configuration itself featured eight measuring points, while the triangle with flare configuration had 14. Notably, the eight measuring points of the triangle configuration are common to the triangle with flare configuration.

A comprehensive examination of the pressure results reveals the following distinctions between the top row flare (Configuration 1) and flare with ski jump (Configuration 2):

- The top row flare option (Configuration 1) recorded the most negative pressures across the range of flow rates tested, with 200 m³/s/m unit discharge exceeding the 7 m limit.
- The flare with ski jump (Configuration 2) performed the worst at a flow rate of 100 m³/s/m, with the lowest pressure close to the -7 m threshold.
- The addition of the ski jump in Configuration 2 influenced the pressures on the half top row flare (Configuration 1). This could be due to contraction effects.

A comparative analysis between the triangle (Configuration 3) and triangle with flare (Configuration 4) reveals several key findings:

- The triangle (Configuration 3) had a single negative pressure reading solely at the 50 m³/s/m unit discharge, with all higher flow rates yielding no negative readings. This may be due to scale effects.
- The triangle with flare (Configuration 4) had low pressures that could result in cavitation for the unit discharge of 50 m³/s/m. However, all flows above 50 m³/s/m exhibit no such issues.
- The triangle with flare (Configuration 4) had one negative pressure reading for the unit discharge of 100 m³/s/m. All flows above this had no negative readings.
- The deflection achieved by the triangle with flare (Configuration 4) contributed to more significant positive pressures at the bottom of the triangle located closest to the side flare. However, this phenomenon is not consistent for the same positions, located closest to the centre flare.
- The pressures at the top of the triangle, in the middle between the flares, were higher for the triangle with flare (Configuration 4) than for the triangle (Configuration 3).

The flare with ski jump (Configuration 2) and triangle (Configuration 3) performed the best at all the flows. The triangle with flare (Configuration 4) did not meet the cavitation threshold criteria for the unit discharge of 50 m³/s/m due to scale effects, while the top row flare (Configuration 1) did not meet the unit discharge of 200 m³/s/m. Table 8 summarises where the various deflectors meet the threshold criteria.

Among the deflector configurations, the flare with ski jump (Configuration 2), triangle (Configuration 3) and triangle with flare (Configuration 4) options exhibited the most significant deflection away from the spillway slope. In contrast, the flare (Configuration 1) displayed the least deflection.

The jet trajectory for the different deflector configurations compared to that of the top row flare (Configuration 1) decreased with an increase in discharge, as shown in Table 9. Furthermore, it was noted that the triangle with flare (Configuration 4) had the greatest difference compared to Configuration 1, and the triangle (Configuration 3) the least. The flare with ski jump (Configuration 2) had a larger trajectory than the triangle (Configuration 4) at discharges of 50 m³/s/m and 200 m³/s/m, but both were similar for flows of 100 m³/s/m and 150 m³/s/m due to drowning of the jet. The spread in the jet, i.e. from inside to outside, is similar for the various configurations, although the flare with ski jump (Configuration 2) indicates the largest variation due to aeration or flow bulking.

Table 10 Safe spillway length prototype

Deflector	Safe spillway length (m)			
	q = 50 $m^3/s/m$	q = 100 $m^3/s/m$	q = 150 $m^3/s/m$	q = 200 $m^3/s/m$
Top row flare (Configuration 1)	35.30	54.80	89.50	93.75
Flare with ski jump (Configuration 2)	114.65	124.50	124.50	134.65
Triangle (Configuration 3)	104.50	125.40	123.00	123.55
Triangle with flare (Configuration 4)	123.90	153.50	155.80	163.50

The physical model design of the stepped spillway implemented 160 steps related to a spillway length of 235 m along the slope. The spillway length from the deflector bottom to the position upstream where the flow meets the downstream slope herein was deemed to be the 'safe spillway length'. The pressure at this impact zone was not measured but was aerated, as seen from the visual observations. Table 10 shows the safe spillway length for each deflector configuration as prototype values. This was based on the jet trajectories measured in the physical model. The triangle with flare (Configuration 4) had the longest safe distance for all flows, whereas the top row flare (Configuration 1) had the least safe distance. As the discharge increased, the safe distance increased, except for the triangle (Configuration 3), where submergence of the jects occurred.

CONCLUSION

A 3D physical model (based on Froude scale laws) of a 200 m high dam was constructed. The physical model consisted of an elevated approach, a steel ogee section, and wood steps with a slope of 0.8 H: 1.0 V. A model scale of 1:50 was chosen for the experimental results from this study to limit scale effects, although some scale effects were apparent for flows of less than 80 $m^3/s/m$. The constructed scaled physical model was used to observe the flow patterns under a range of flow conditions and to collect pressure and jet trajectory data for various deflector forms.

Among the deflector configurations, the flare with ski Jump (Configuration 2), the triangle (Configuration 3) and the triangle with flare (Configuration 4) options exhibited the most significant deflection away from the spillway slope. In contrast, the top row flare (Configuration 1) displayed the least deflection. Based on the pressure threshold of -7 m, the flare with ski jump (Configuration 2) and triangle (Configuration 3) performed the best at all the flows. The triangle with flare (Configuration 4) did not meet the cavitation threshold criteria for the unit discharge of 50 $m^3/s/m$ (due to scale effects), while the top row flare (Configuration 1) did not meet the criteria for the unit discharge of 200 $m^3/s/m$. When a trajectory criterion of a minimum of 100 m is added, the triangle (Configuration 3) and the triangle with flare (Configuration 4) performed the best. If the jet trajectory criterion is increased to 150 m, only the triangle with flare (Configuration 4) meets the threshold for flows above 100 $m^3/s/m$.

The experimental results showed that the flow rate and geometry of the deflectors affected the pressures and jet trajectory. While the jet trajectory generally increased as the flow increased, submergence of the deflector was apparent in some cases, which decreased the jet trajectory.

The various deflector geometries, as explored in this study, demonstrated favourable performance in terms of deflection distance when compared to other established deflectors, such as Roberts' splitters and trajectory buckets. While stepped spillways effectively dissipate energy at moderate discharges, their performance diminishes at higher flow rates, necessitating alternative solutions. The deflectors introduced in this study provide a means to safely handle unit discharges exceeding 50 $m^3/s/m$, where conventional stepped spillways would no longer be viable without additional aeration or modification. Novel deflectors were designed that can potentially be used for high head dams (> 100 m) for flow rates up to 200 $m^3/s/m$; notably the triangle (Configuration 3) for heights up to 130 m and the triangle with flare (Configuration 4) for heights above 150 m. However, while these results suggest potential as effective alternatives in hydraulic design, the implementation of deflectors must be carefully evaluated on a case-by-case basis. Site-specific factors, such as energy dissipation requirements, cavitation potential, and structural loading, should be thoroughly assessed before practical application. Further research, including numerical modelling and prototype-scale studies, is recommended to refine the deflector designs and validate their effectiveness under real-world conditions. In particular, additional investigations should focus on quantifying energy dissipation efficiency, mitigating cavitation risks through optimised deflector geometry, and verifying scale effects through larger-scale physical or field studies. While this study provides a solid foundation, site-specific evaluations will be necessary to ensure the safe and effective application of deflectors in practical spillway designs.

Although deflectors alter the flow trajectory, the experimental results confirm that the flow is effectively directed away from the spillway slope without excessive increase in downstream velocity. Additionally, in practical applications, tailwater depth at the spillway toe will further contribute to energy dissipation and erosion control.

In practice, the apexes of such deflectors would likely have to be fitted with stainless steel caps with a flat top (or similar) to prevent damage or cracking due to high-velocity flow, temperature variations, and impact loads from floating debris. While large sediment loads are generally not expected due to reservoir sedimentation, fine suspended material may occasionally be present during extreme flood events. Additionally, localised wear could occur due to turbulence, cavitation, or debris impact. These protective measures are necessary to ensure the longevity and durability of the deflectors under operational conditions.

Although this study primarily focused on the hydraulic performance of deflectors, future research should investigate their structural implications in greater detail. This includes assessing potential stress concentrations, reinforcement requirements, and long-term durability under extreme flow conditions. Additionally, further studies should evaluate the interaction

between deflected jets and downstream flow conditions, including potential erosion effects at the spillway toe and the influence of tailwater depth. A comprehensive structural analysis will further ensure that deflector designs maintain both hydraulic efficiency and structural integrity.

ACKNOWLEDGEMENTS

The assistance of the Stellenbosch University Hydraulic Laboratory personnel, namely Johann Niewoudt, Guillaume Nel, Iliyaaz Williams, and Jody February, as well as Prof Gerrit Basson, is acknowledged with gratitude. The opinions expressed and conclusions arrived at are those of the authors.

REFERENCES

Amador, A, Sánchez-Juny, M & Dolz, J. 2009. Developing flow region and pressure fluctuations on steeply sloping stepped spillways. *Journal of Hydraulic Engineering*, 135(12):1092–1100.

Back, P A A, Frey, J P & Johnson, G. 1973. PK le Roux Dam spillway design and energy dissipation. *Proceedings*, 11th Congress of the International Commission on Large Dams, Madrid, pp 1439–1468.

Boes, R M. 2012. Guidelines on the design and hydraulic characteristics of stepped spillways. *Proceedings*, 24th Congress of the International Commission on Large Dams, Kyoto, pp 203–220.

Boes, R M & Minor, H E (Eds). 2000. Guidelines for the hydraulic design of stepped spillways. *Proceedings*, International Workshop on Hydraulics of Stepped Spillways, Rotterdam, pp 53–60.

Boes, R M & Hager, W H. 2003. Two-phase flow characteristics of stepped spillways. *Journal of Hydraulic Engineering*, 129(9): 661–670.

Calitz, G & Basson, G R. 2018. The effect of aeration through an internal gallery of a dam on the cavitation risk of Roberts splitters. *Journal of the South African Institution of Civil Engineering*, 60(1): 31–43.

Chadwick, A, Morfett, J & Borthwick, M. 2013. *Hydraulics in Civil and Environmental Engineering*. CRC Press.

Chanson, H. 1989. Study of air entrainment and aeration devices. *Journal of Hydraulic Research*, 27(3): 301–319.

Chanson, H. 1994. Aeration and deaeration at bottom aeration devices on spillway. *Canadian Journal of Civil Engineering*, 21(3): 404–409.

Chanson, H. 2002. *Hydraulics of stepped chutes and spillways*. Rotterdam, CRC Press.

Chanson, H. 2009. Turbulent air-water flows in hydraulic structures: dynamic similarity and scale effects. *Environmental Fluid Mechanics*, 9(2):125–142.

Chanson, H. 2015. *Energy dissipation in hydraulic structures*. London, CRC Press.

Falvey, HT. 1990. *Engineering Monograph No. 42: Cavitation in chutes and spillways*. Denver, CO: United States Department of the Interior. Bureau of Reclamation.

Frizell, K W, Renna, F M & Matos, J. 2013. Cavitation potential of flow on stepped spillways. *Journal of Hydraulic Engineering*, 139(6): 630–636.

Geringer, J J & Officer, A K. 1995. Stepped spillway hydraulic research for RCC dams – Quo Vadis? *Proceedings*, International Symposium on Roller Compacted Concrete Dams, Santander, pp 549–563.

Geringer, J J. 1995. The design and construction of RCC dams in Southern Africa. *Proceedings*, International Symposium on Roller Compacted Concrete Dams, Santander.

Geringer, J, Nazzal, M & Salojee, A. 2012. Spillway and Energy Dissipation Design Considerations for Metolong Dam. *Proceedings*, 24th Congress of the International Commission on Large Dams, Kyoto.

Guo, J, Liu, Z & Ly, Y. 2003. Field observations on the RCC stepped spillways with the flaring pier gate on the Dachaoshan project. *Proceedings*, 30th IAHR Biennial Congress, Thessaloniki, pp 473–478.

Guo, J. 2012. Recent achievements in hydraulic research in China. In *Comprehensive Renewable Energy*, Vol 6. Elsevier: 485–505.

Hager, W H & Boes, R M. 2014. Hydraulic structures: a positive outlook into the future. *Journal of Hydraulic Research*, 52(3): 299–310.

Hager, W H, Schleiss, A J, Boes, R M & Pfister, M. 2021. *Hydraulic Engineering of Dams*. CRC Press.

Heller, V, Hager, W H and Minor, H E. 2005. Ski jump hydraulics. *Journal Of Hydraulic Engineering*, 13(5): 347–355.

ICOLD. 1992. Spillways, shock waves and air entrainment. In *ICOLD Bulletin 81*. Paris: International Commission on Large Dams (ICOLD).

ICOLD. 2017. Technical advancements in spillway design: progress and innovations from 1985 to 2015. In *ICOLD Bulletin 172*. Paris: International Commission on Large Dams (ICOLD).

Ji, J W K, Kien, T K & Hing, S H. 2014. 1:40 scale model study of the 120 m-high stepped spillway design for Murum hydroelectric project in Sarawak, Malaysia. *Proceedings*, Hydro 2014, Cernobbio.

Khatsuria, R M. 2005. *Hydraulics of spillways and energy dissipators*. New York: Marcel Dekker.

Koen, J. 2017a. *Artificial aeration of stepped spillways with piers and flares to mitigate cavitation damage*. MSc thesis. University of Stellenbosch.

Koen, J. 2017b. Large unit discharge stepped spillway designs with crest piers and flares. *Proceedings*, SANCOLD Annual Conference 2017, Tshwane: 69–78.

Lin, B, Li, G & Chen, H. 1987. Hydraulic research in China. *Journal of Hydraulic Engineering*, 113(1): 47–60.

Lopardo, R. 2002. Contribution of hydraulic models on the safe design of large dams stilling basins. *Proceedings*, IAHR Symposium on Hydraulic and Hydrological Aspects of Reliability and Safety Assessment of Hydraulic Structures, St. Petersburg.

Mason, P J. 1983. Energy Dissipating Crest Splitters for Concrete Dams. *Water Power & Dam Construction*, 35(11), 37–40.

Mason, P J. 1993. Practical guidelines for the design of flip buckets and plunge pools. *Water Power & Dam Construction*, 45(9-10), 40–45.

Matos, J & Meireles, I. 2014. Hydraulics of stepped weirs and dam spillways: engineering challenges, labyrinths of research. In *ISHS 2014 Hydraulic Structures and Society – Engineering Challenges and Extremes: Proceedings*, 5th IAHR International Symposium on Hydraulic Structures, Brisbane, pp 1–30.

Minor, H E. 2000. Spillways for high velocities. *Proceedings*, International Workshop on Hydraulics of Stepped Spillways, Rotterdam, pp 3–10.

Nan, F & Rumyantsev, I. 2014. Modeling of flood routing through stepped spillway of water reservoir dam. *Proceedings*, 11th International Conference on Hydroinformatics, New York.

Peterka, A J. 1953. The effect of entrained air on cavitation pitting. *Proceedings*, Minnesota International Hydraulic Convention, Minneapolis, pp 507–518.

Pfister, M & Chanson, H. 2014. Two-phase air-water flows: Scale effects in physical modeling. *Journal of Hydrodynamics, Ser. B*, 26(2): 291–298.

Pfister, M, Hager, W H and Minor, H E. 2006a. Bottom aeration of stepped spillways. *Journal of Hydraulic Engineering*, 132(8): 850–853.

Pfister, M, Hager, W H and Minor, H E. 2006b. Stepped chutes: Pre-aeration and spray reduction. *International Journal of Multiphase Flow*, 32(2): 269–284.

Pietrangeli, G, Bezzi, A, Beltrami, G M and Marfur S. 2018. Grand Ethiopian Renaissance dam project: Stepped spillway design. *Proceedings*, 2018 Hydropower and Dams Conference. Gdansk.

Roberts, C P R. 1977. Energy dissipation by dam crest splitters. *Civil Engineering*, 1997(11): 263–264.

Saayman, R L. 2020. *Energy dissipation at uncontrolled high dam spillways by flares*. MSc thesis. University of Stellenbosch.

Schleiss, A J. 2002. Scour evaluation in space and time – the challenge of dam designers. *Proceedings*, International Workshop on Rock Scour Due to Falling High-velocity Jets, Lausanne, pp 3-22.

SANCOLD. 2016. *South African Large Dams – A century of engineering innovation*. South African National Committee on Large Dams (SANCOLD) & Water Research Commission.

Sudol'skii, G A & Volynchikov, A N. 2017. Testing the Stepped Spillway of the Boguchany Dam. *Power Technology and Engineering*, 50(6): 567–571.

Terrier, S. 2016. *Hydraulic performance of stepped spillway aerators and related downstream flow*

features. PhD thesis. Ecole Polytechnique Fédérale de Lausanne.

Toloshinov, A V, Volynchikov, A N, Prokof'ev, V A, & Sudol'skii, G A. 2009. Development of the design for the No. 2 spillway at the Boguchany hydroproject. *Power Technology and Engineering*, 43(3): 135–142.

Vischer, D L & Hager, W H. 1995. *Energy dissipators*. Rotterdam.

Wang, S Y, Hou, D M, & Wang, C H. 2012. Aerator of stepped chute in Murum Hydropower Station. *Procedia Engineering*, 28: 803–807.

Willey, J, Ewing, T, Lesleighter, E & Dymke, J. 2010. Refinement of the hydraulic design of a complex stepped spillway through numerical and physical modelling. *Proceedings*, ASIA 2010 Conference, Sarawak.

Wright, H J. 2006. *Protrusions on Stepped Spillways to Improve Energy Dissipation*. MSc thesis. Stellenbosch University.

Wright, H J. 2010. Improved energy dissipation on stepped spillways with the addition of triangular protrusions. *Proceedings*, 78th Annual Meeting and Symposium of the International Commission on Large Dams, Hanoi.

Wright, H J and Cameron-Ellis, D G. 2018. Energy Dissipation Provisions for Stepped Spillways: Are Additional Measures Necessary? A Southern African Perspective. *Proceedings*, SANCOLD Annual Conference 2018, Somerset West, pp 245–255.

Zamora, A S, Pfister, M & Hager, W. 2008. Hydraulic performance of step aerator. *Journal of Hydraulic Engineering*, 134(2): 127–133.

APPENDICES

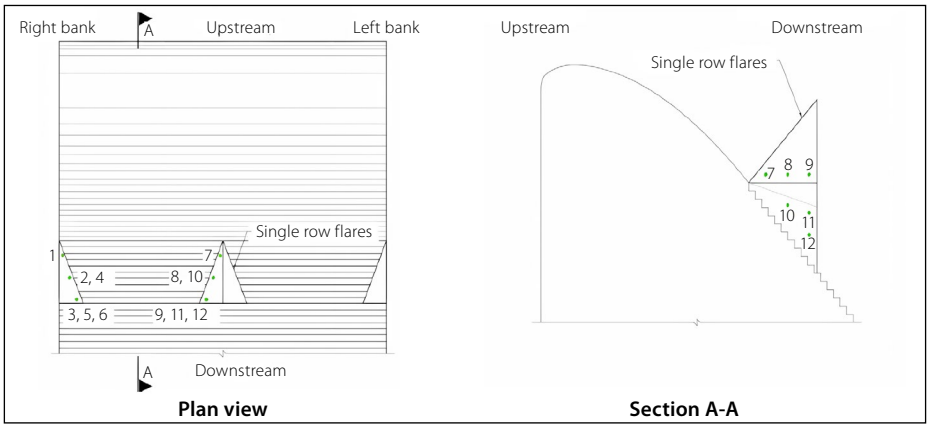

Figure A1 Top row flare pressure measurement positions

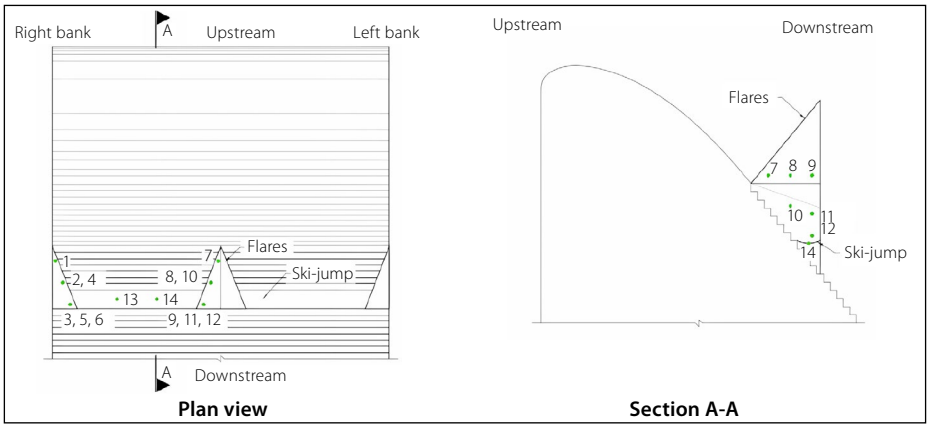

Figure A2 Flare with ski jump pressure measurement positions

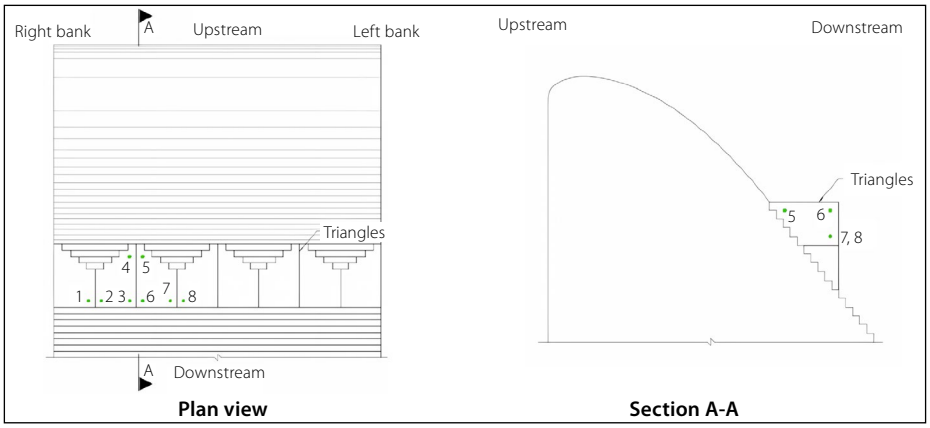

Figure A3 Triangle pressure measurement positions

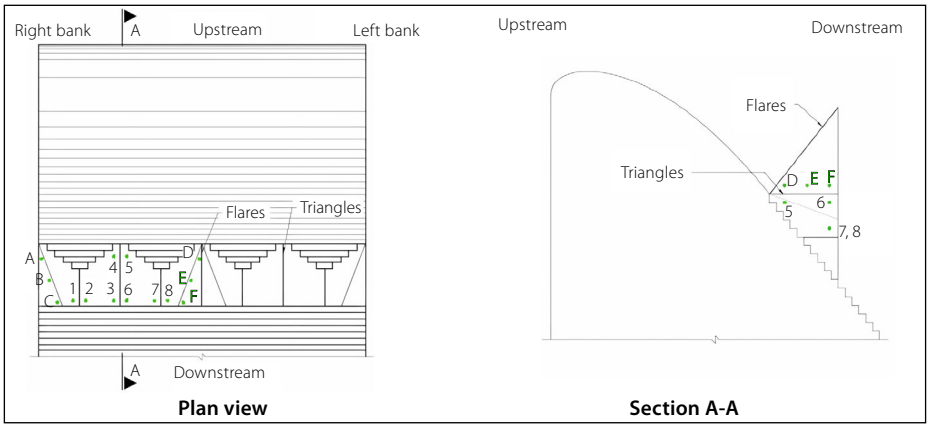

Figure A4 Triangle with flare pressure measurement positions

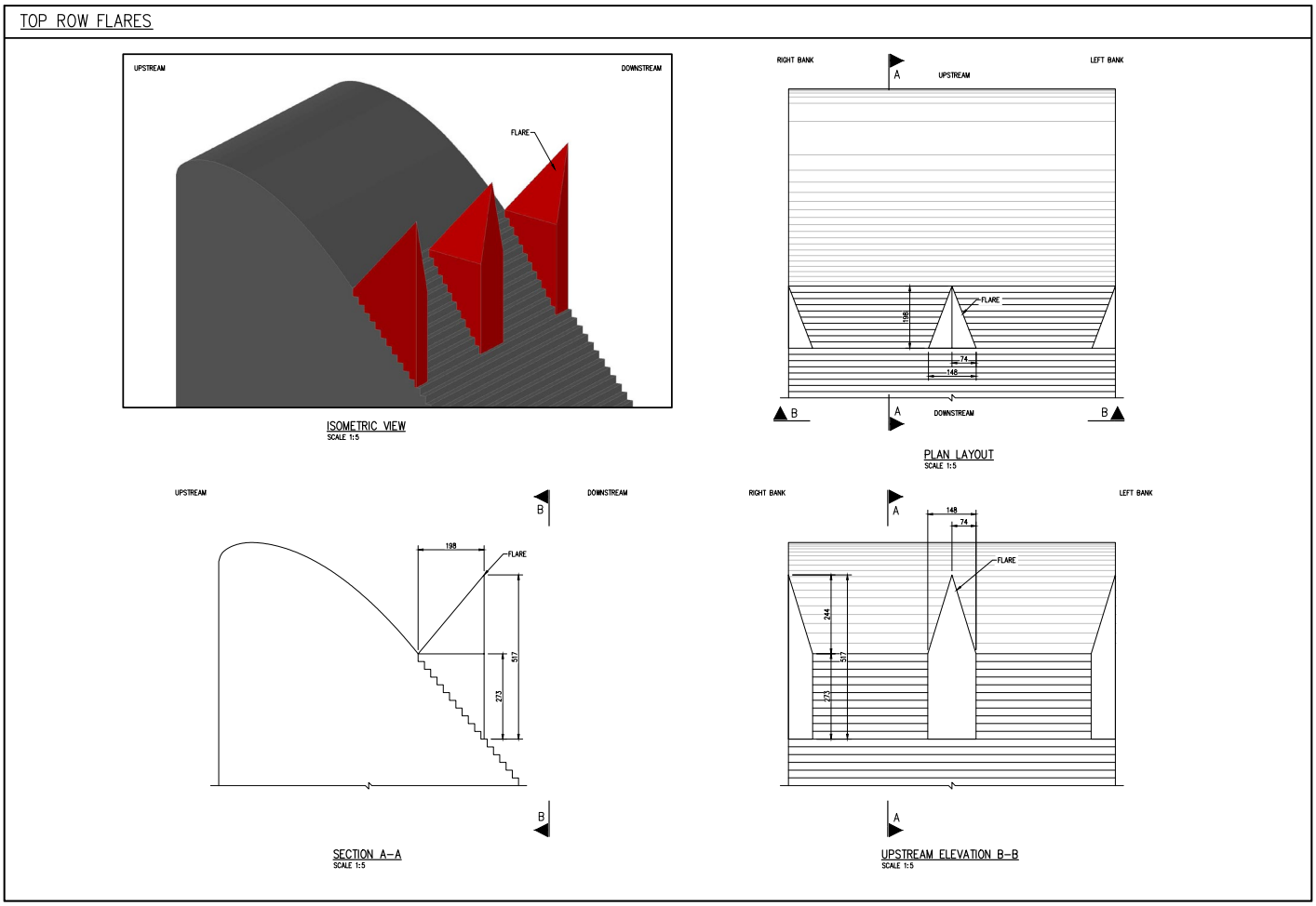

Figure B1 Top row flare dimensions

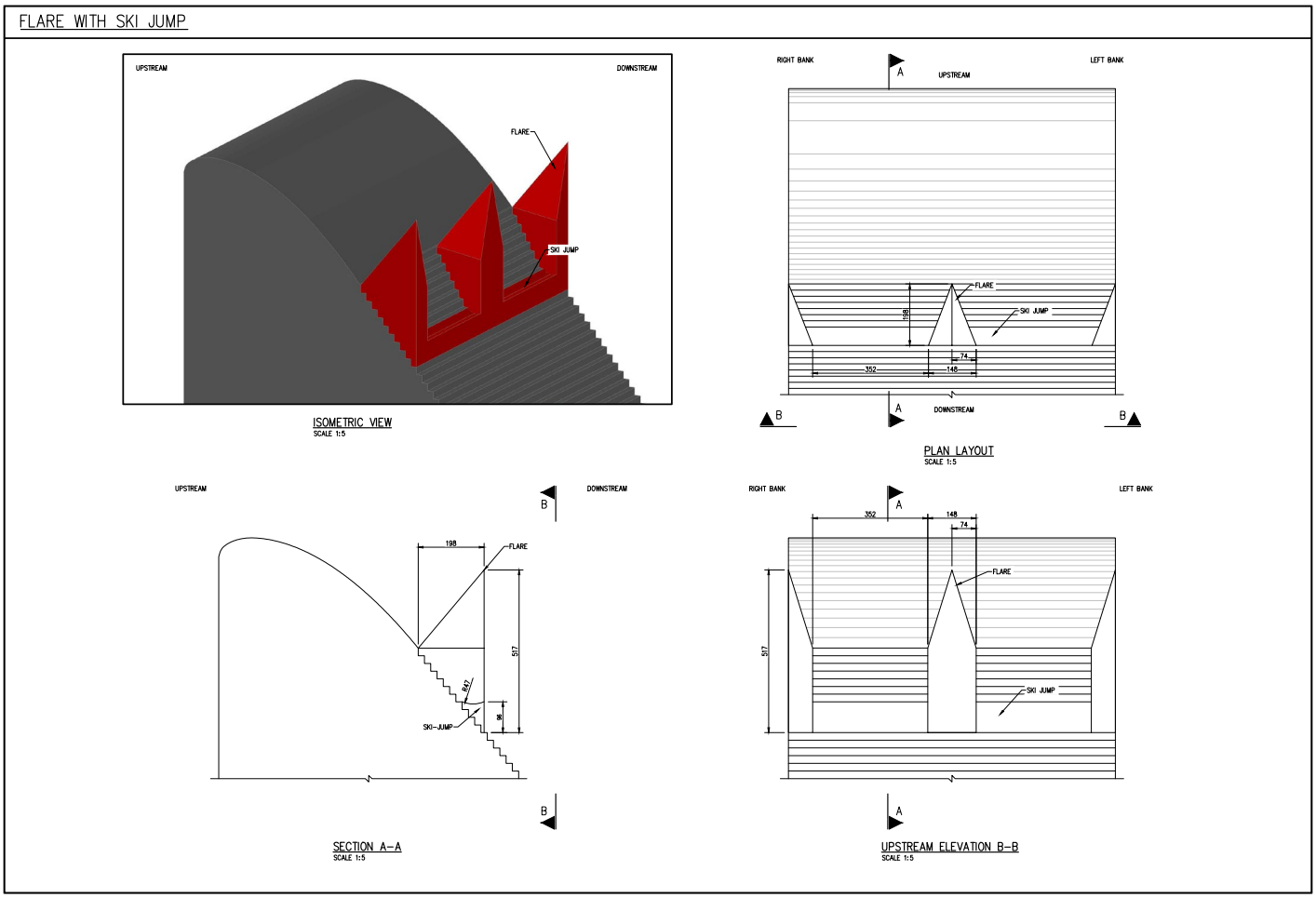

Figure B2 Flare with ski jump dimensions

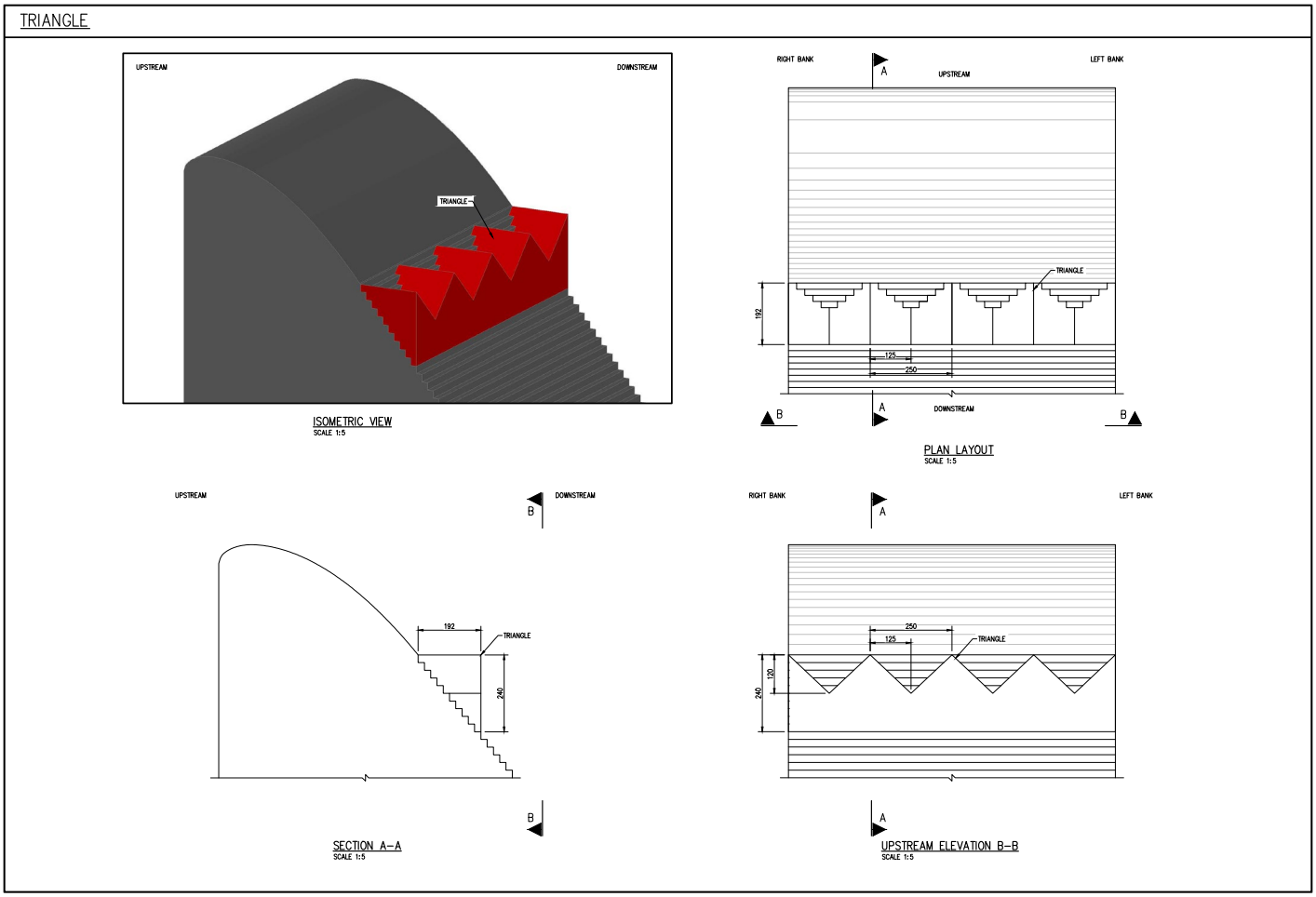

Figure B3 Triangle dimensions

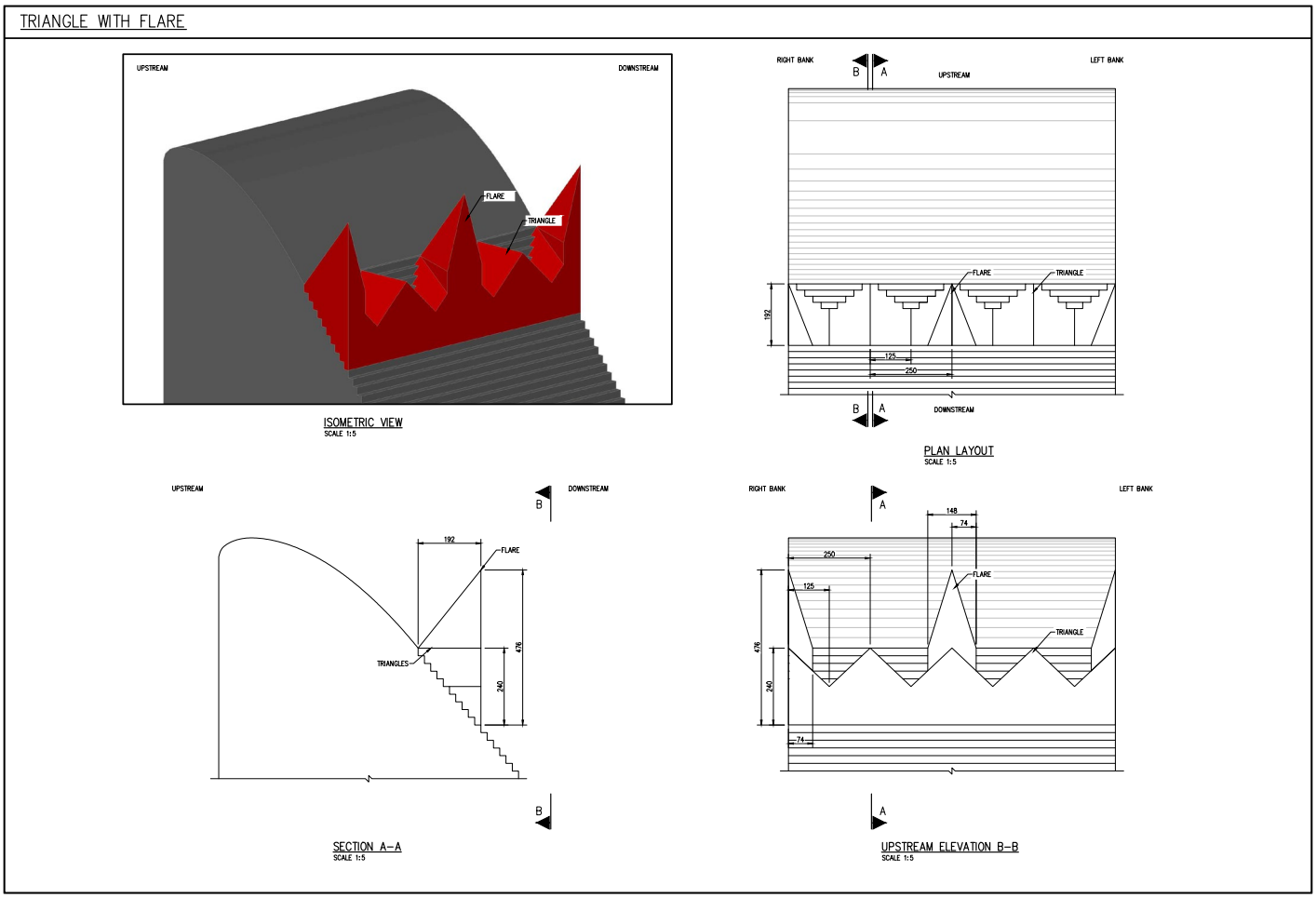

Figure B4 Triangle with flare dimensions